International Journal of Mechanical and Production Engineering Research and Development (IJMPERD)
ISSN (P): 2249-6890; ISSN (E): 2249-8001
Vol. 8, Issue 1, Feb 2018, 373-388

THE EFFECTS OF TiC REINFORCEMENT ON THERMAL, ELECTRICAL AND DRY SLIDING WEAR BEHAVIOUR OF ALUMINIUM MATRIX NANOCOMPOSITES

M. SIVARAJ[1], S. MUTHURAMAN[2], N. SELVAKUMAR[3] & S. RAJKUMAR[4]

[1, 4] *School of Mechanical and Electro Mechanical Engineering, Hawasaa University, Hawasaa, Ethopia*

[2] *Department of Mechanical Engineering, Higher College of Technology, Muscat, Oman*

[3] *Department of Mechanical Engineering, Mepcoschlenk Engineering College, Virudhunagar, Tamilnadu, India*

ABSTRACT

The present work is to investigate the thermal, electrical & dry sliding wear behaviour of aaluminium matrix composite reinforced with dissimilar particle size (≤ 200 nm and 2 µm) of titanium carbide particles. An aluminium matrix composite with 0, 5, 10 and 15 vol.%TiC reinforcement was prepared by using powder metallurgy. A pin-on-disc apparatus was broadly used to investigate the wear behavior of the Al/TiCnano composites. Wear test was carried out for normal load of 5 N,10 N, 15 N& 20N at constant sliding velocity of 2.61 m/s at room temperature. The variations of the coefficient of friction (COF) & specific wear rate (SWR) with the varying sliding distances (1000 m, 1200 m, 1400 m and 1600 m) for variable load were plotted and analyzed. Find out the thermal property of Al-TiC composite by using Thermogravimetry (TG) / Differential scanning calorometry (DSC). To study the dominant sliding, wear mechanism was analyzed for various test condition, while the worn surface was investigated by using scanning electron microscopy (SEM) and the respective polynomial & power law model was developed using curve fitting technique. Further, it was found that the SWR is to increase with the load & sliding distances. Hardness & electrical conductivity of composites have been varied based on particle size variation of TiC.

KEYWORDS: Dry Sliding Wear; Nanocomposite; Friction; Nano-reinforcement; Worn Surface & Thermogravimetry

Received: Nov 21, 2017; **Accepted**: Dec 12, 2017; **Published**: Jan 06, 2018; **Paper Id**.: IJMPERDFEB201841

Original Article

INTRODUCTION

Aluminium alloys reinforced with SiC and Titanium Carbide (TiC) particles were broadly used for manufacturing mould, die, automotive, aerospace and surgical components by virtue of high specific strength and elevated temperature resistance. However, the full potential of these metal matrix composites is hindered by cost effectiveness and difficulties in machining process which generally result in excessive tool wear due to the abrasive nature of the material [1]. Ceramic particles-reinforced aluminium MMCs fabricated by P/M processes were also being extensively studied due to their potential low fabrication cost. TiC particle reinforced MMCs are very much interesting, because of the thermodynamically stable nature of TiC and enhances the hardness and lightness of the composite [2].

Many of the investigations were focused on friction and wear properties of the MMCs [3-5]. The principal tribological parameters that control friction and wear properties of MMCs can be classified into two levels, namely mechanical (extrinsic factor) and material (intrinsic factor) [6]. Among these factors, the effects of applied load,

atmosphere temperature and reinforcement contents on friction and wear properties of MMCs have been investigated by many researchers [7-8]. Choh [9] fabricated in situ TiC composite by utilizing the reaction between liquid aluminium alloy containing thermodynamically stable carbide forming elements and relatively unstable carbide such as SiC and Al_4C_3 as solid reaction sources.

Roy et al.[10] have studied sliding wear behaviour of Al matrix composites reinforced with SiC, TiC, TiB_2, B_4C particles and noted that the composite has lower wear rates and coefficient of friction as compared to the pure aluminium. It has been also noted that many key factors such as type, size and volume fraction of particles as well as the interfacial particle/matrix bonding have a pronounced influence on the wear behavior of composites reinforced with in situ particles. Nanosizedaluminium powder in the flash powder exhibits high thermal energy content and high sensitivity in various compositions of flash powder. The thermal behavior studies in the above work were analyzed by DTA/TG and DSC [11,12]. Safety analysis was conducted for Synthesizednanoaluminium and titanium powders [13]. Nanoparticles have a greater thermal behavior while compared with micron sized powder [14].

Even though the wear rate and friction rely upon many factors such as applied load, environmental temperature, specimen geometry, surface roughness, sliding speed, material type, sliding distance, relative humidity and system rigidity, it has been found that sliding distance and normal load had a particulate strong effect on the wear rate [15,16]. Based on this context, in the present work various parameters of Al/TiC nanocomposites was studied i.e, conductive and dry sliding wear behavior, thermal analysis, electrical conductivity, wear rate, coefficient of friction, the effect of load and sliding distance on the wear behaviour.

EXPERIMENTAL PROCEDURE

Material

Aluminum powder with an average particle size of 40 $\mu m$and 99.8% purity were used as the matrix material. TiC powder with an average particle size of 2 μm and 99.6% purity were supplied from Alfa AesarPvt Ltd, England. The characteristics of the aluminium and TiC powders were shown in Table 1(a-b).

Table 1(a): Aluminium Powder Characteristics

	Sieve Size (μm)	Wt.%
Aluminium	+106	00.26
	+90	02.54
	+75	14.73
	+63	17.58
	+53	24.86
	+45	12.33
	+38	06.27
	-38	21.42
Apparent density ($g.\ cm^{-3}$)		1.030
Flow rate, (by Hall flow meter) ($50g^{-1}$)		32.00
Particle size-dry sieve test standard		ASTM B-214

Table 1(b): Titanium Carbide Powder Characteristics

Purity %	99.5
Sieve size (μm)	2
Density ($g.\ cm^{-3}$)	4.93
Melting point ^0C	3,140

Powder Preparation

The TiC powder was pulverized to below 200 *nm*and and was obtained by using high-energy planetary ball mill for 13*h,* with the speed of 150 rpm. The individual powders (Al, TiC) were fine-grained in a planetary ball mill using tungsten carbide grinding medium. The ball to powder ratio was 1:20 and liquid acetone was used as a process control agent. Further 1.5 *h* and later it was blended on a mass basis with 0, 5, 10 and 15%titanium carbide and rest aluminium powder. Then the combined Al/TiC powders were mixed scientifically in the high energy ball mill for another 0.25 *h* to attain homogeneous mixture [17].

Composite Preparation

Compacting

Specimens were prepared using different particle size of TiC namely ≤ 200*nm&2µm* with 10 *mm* diameter &30 *mm* height through powder metallurgy technique at a compaction pressure of 675 *MPa*. This was compacted by compression testing machine (2.0 *MN)* by using die assembly. Zinc-sterate was used to lubricate the die set, the density variation was maintained by mass & compacting pressure.

Sintering

After compaction, the preforms were removed from the die set carefully and loaded into the furnace for sintering. The sintering was carried out in a vacuum furnace (to prevent oxidization) at 575±5^{0}C for a period of 1.5 h. After that the sintered preforms were left in the furnace for cooling until it reaches its room temperature. After sintering, the specimens were cleaned further by wire brush.

Density

Experimental density was determined by the Archimedes method[18] and the theoretical density was calculated from the simple rule of mixtures. The amount of relative density increases with particle size reduction of TiC content.

Composite Characterization

Microscopy

A Microstructural characterization study was conducted on metallographically polished samples to investigate morphological characteristics of grains and presence of second phases and worn surface after wear test by using Scanning Electron Microscope (SEM). Field Emission Scanning Electron Microscope (FESEM) was used to confirm the uniform distribution of reinforced particles.

X-Ray Diffraction

The composite sample was examined by X-ray diffraction (XRD) using Cu-$k_\alpha$radiation with a wavelength of 1.54056A^0over a 2θ range of 20–90$^\theta$. In order to detect the Al, TiC and any oxide of Al and TiC particles, Energy Dispersive Spectroscopy (EDS) analyses were performed.

Thermal Analysis

Thermal analysis of Al/TiC preforms was carried out by Perkin Elmer PhyrisThermogravimetry (TG). Thermal activity was analyzed at the heating rate of $32^0C\ min^{-1}$ in nitrogen atmosphere between temperature range of 100 to 1000^0C of Al_2O_3 crucible.

DSC was used for finding out the melting, crystallization and ignition behavior of the composites. The thermal degradation behavior of the Al-5TiC (2μm) and Al-5TiC (≤200 nm) composite were studied by TGA. The information about the thermal stability and extent of degradation of materials were taken from the integral of TGA and derivative DSC curves [19].

Hardness

Hardness of composites was determined using a Vickers indentation technique with a load of 500*g* dwelling for 10-15*s* at room temperature and the values were shown in Table 2.

Table 2: Vickers Hardness of Sintered Samples

Hardness values (*Hv*) 500*g*,10*s*, Material Al-5TiC	
≤200*nm*	2*μm*
41.5	34.5
44.6	36.4
45.6	36.2

Electrical Conductivity

Eddy current instruments in accordance with ASTM standard E1004-02 were used for finding out the electrical conductivity of Al/TiC composites [20]. The electrical conductivity of Al/TiC was determined by this equipment was usually stated as a percentage of the conductivity of the International Annealed Copper Standard (% IACS).

Wear Test

The entire experiment was performed in air at $(30\pm1)^0C$along with ASTM: G99-04 in DUCOM TR20-LEpin-on-disc wear testing machine [21]. The contact surface of the specimens was polished by a variety of grid/emery papers (800, 1000, 1200 microns). The prepared pin samples were set in the slot arm above the rotating disc. The surface contact between the sample & disc surface were reserved at 100%. An electronic balance having a resolution of 0.0001 g was used to measure the weight loss. The experiment was done with normal load of 5, 10, 15 & 20*N* at constant velocity of 2.61 *m/s* on the disc surface with varying sliding distance of 1000, 1200, 1400 & 1600 *m,*& four different TiC weight fractions (0%, 5%, 10%, & 15%). At the end of every sliding distance interval, the pin was carefully cleaned using acetone to remove the burrs developed during the sliding of the pin on the disc surfaces. The exact mass of the pin was measured after the removal of wear debris from pin surface, and the mass loss was calculated at each sliding distance interval. All of the worn pin surface was analysed using SEM to study the dominant wear behavior.

RESULTS AND DISCUSSIONS

Microstructure and Phase Analysis

SEM was used for the assessment of particles before & after milling exhibited Figure 1(a-d). Figure 1(a) the aluminium particles shows sphere-shaped & cubic shaped. Figure 1(b) shows the TiC particles have the shape of a starch and pancake. Father Figure 1 (c) illustrates the TiC extremely fine particles after milling of ten hours. Figure 1(d)

illustrates that TiC mixed with Al powder.

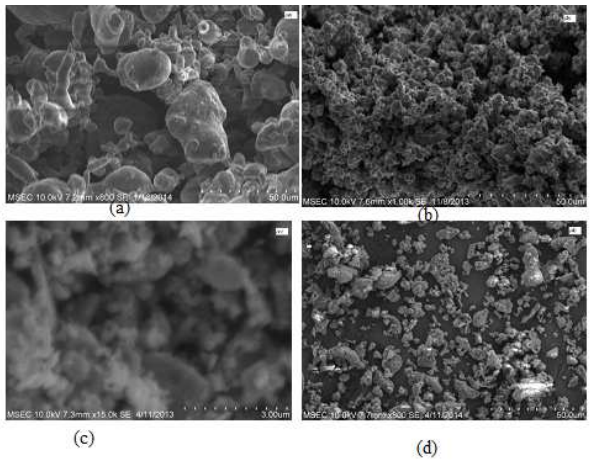

Figure 1: (a-d) SEM Micrograph (a) Pure Al, (b) Pure TiC, (c) Tic, 8 h, (d) Al-5TiC Mixed Powder

The FESEM micrographs of the fabricated aluminium matrix composites were presented in Figure 2(a-b). Common defects such as porosity, slag inclusion are not seen in the micrographs which display the quality of the specimen. A very clear observation of the above micrographs pointed out the even distribution of TiC particles in the aluminium matrix. Al-10%TiC (≤200 *nm*) composites compared to Al-10%TiC (2 *μm*) which illustrates very minor agglomeration.

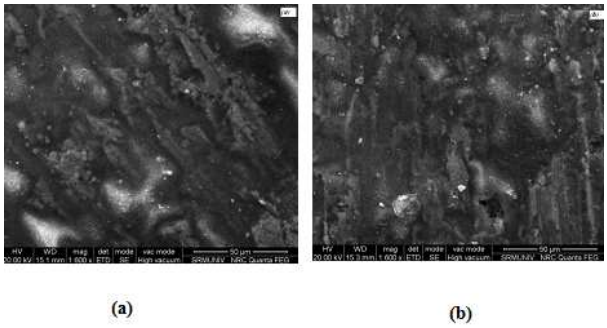

Figure 2: (a-b) FESEM Image of Composite Mixture (a) Al-10TiC (2*μm*) (b) Al-10TiC (≤200*nm*)

Figure (a-b) illustrates X-ray diffraction (XRD) patterns of the aluminum composite reinforced with different TiC particle size. The XRD pattern illustrates two peaks that were identified as Al and TiC. XRD patterns of the composites with TiC particles of different sizes were similar to each other and consist of Al and TiC peaks dominantly to the Face Centred Cubic (FCC) phase of JCPDS file numbers 04-0787 & 32-1383 respectively [22]. Moreover, XRD peak intensities of the TiC phase were increased by reducing particle size of TiC. No oxide peak was observed in the XRD analyses of Al–TiC composites. This suggests that no solid-state reactions between Al and TiC during sintering. This result was very important as far as the electrical conductivity point of view was concerned for related materials [23]. Energy Dispersive Spectroscopy (EDS), Figure 3(c) illustrates the level of aluminum was much higher than that of oxygen in the pure aluminium specimen. Figure 3(d) illustrates the identification of Ti, Al &C particles in the manufactured Al/TiC composite.

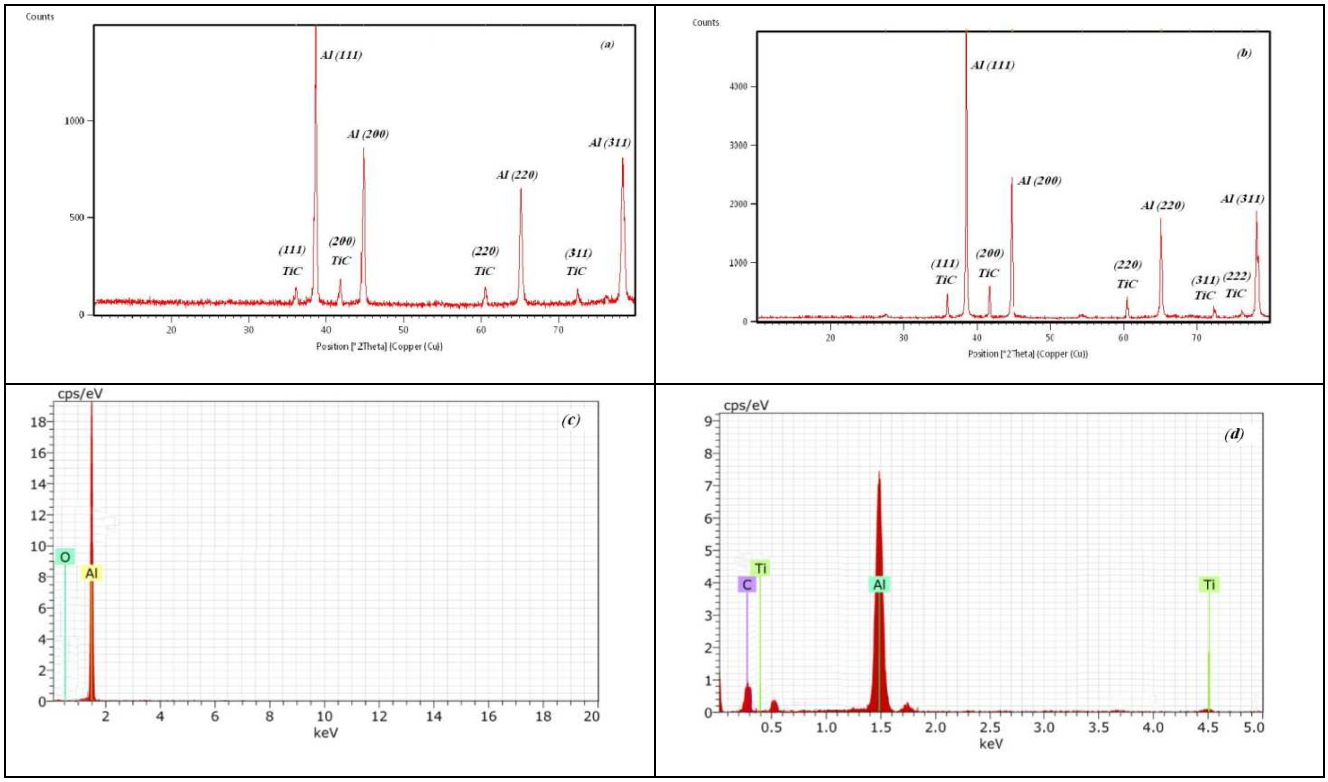

Figure 3: (a-d)XRD Patten of Various Composite (a) Al-5TiC (2μm) (b) Al-5TiC (≤200nm) (c) EDS Spectrum of Aaluminium Composite after Sintering (d) EDS Spectrum of an Al–5TiC Composite after Sintering

Thermal Analysis

In order to understand thermal responses of Al-TiC composites, TG/DSC measurements were performed at the heating rate of $32^0C\ min^{-1}$ in nitrogen atmosphere between temperature ranges of 100^0C to 1000^0C. TG and DSC curves of Al-TiC composites were prepared by powder metallurgy and are depicted in the Figure 4 (a-d).

Figure 4 (a-b) illustrates the DSC interpretation of aluminium composite reinforcement with 2 μm & ≤200 nm TiC particles respectively. The degree of purity of a compound was evaluated by melting point & type of reaction (endo&exo) which was estimated using DSC. Figure 4(a) shows a sharp endothermic peak at about 659.8^0C which indicates the melting and crystalline nature of aluminium matrix Al-5TiC (2 μm) composites. Apart from these there were several other small peaks which indicates to the presence of many sizes of particles. In addition to this, during heating, small particles might be coagulated to larger particles. Figure 4(b) shows a sharp endothermic peak at 660.8^0C indicates melting of the aluminium matrix Al-5TiC (≤200 nm) composites. In the case of nanoparticles reinforced Al metal matrix composites, thermal degradation takes place at higher temperatures than micron size particles. In all DSC samples of metal matrix composites, the degree of purity was observed by employing different particle sizes of TiC. The results indicate the purity, melting heat and temperature for both sizes (2µm, ≤200nm) of particles. Due to the reduction in particle size, thermal degradation takes place with increase in temperature. Further, it was found that during decomposition, the change of enthalpy affects by the particle size reduction of TiC.

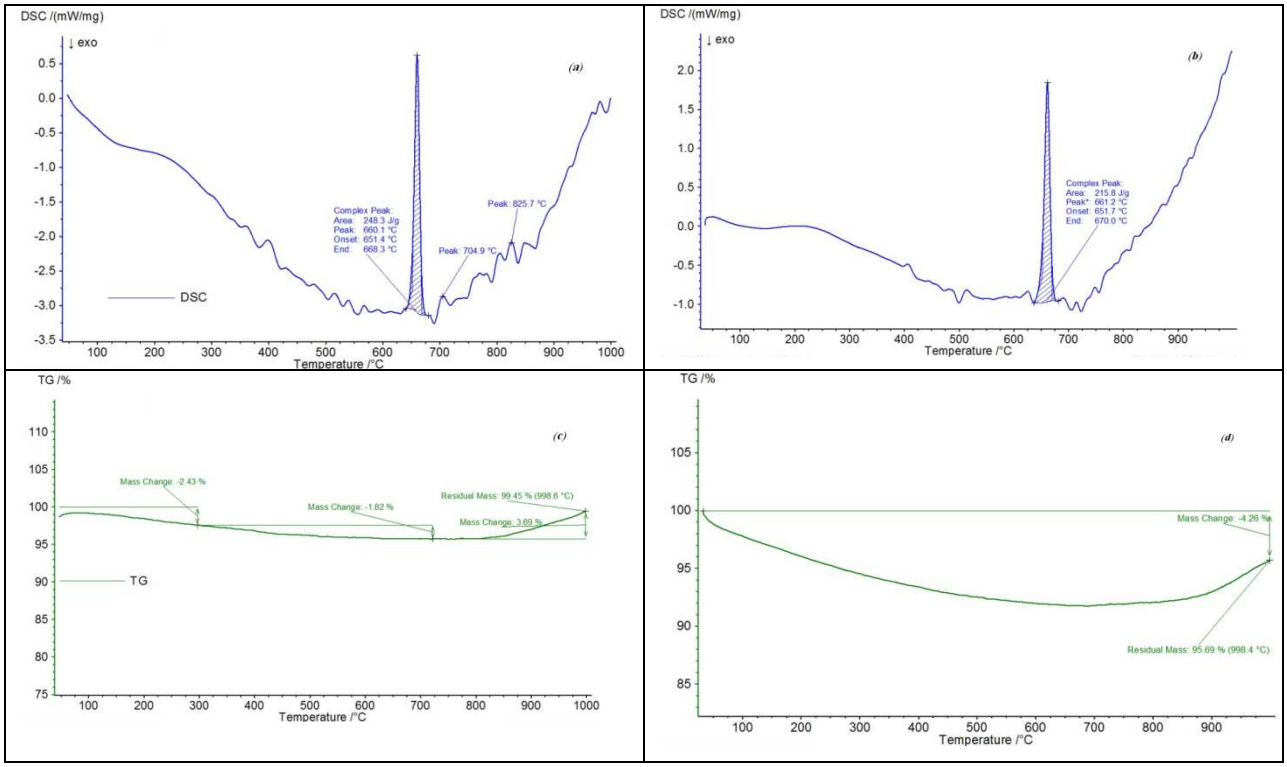

Figuer 4: Thermal Analysis Graph in Al-5TiC (a) DSC of (2 μm), (b) DSC of (≤200 *nm*), (c) TG of (2 μm), (d) TG of (≤200 *nm*)

Figure 4 (c-d) illustrates the TG curves of of aluminium composite reinforcement with 2 μm & ≤ 200 *nm* TiC particles respectively. Figure 4(c) indicates a weight loss in sample upto 825^0C followed by a steady weight gain upto 998.6^0C (2 μm) composites and also Figure 4 (d) indicates weight loss proceeded with less weight gain. Weight loss was attributed to desorption or drying of the sample. Weight gain takes place because of the oxidation reaction of metals by surrounding atmosphere.

$$Al + O_2 \rightarrow Al_2O_3 \tag{1}$$

Based on particle size of the metal matrix composites, Al-5TiC (≤200 *nm*) composites exhibited high weight gain which indicates higher oxidation rate of metal which prevents further chemical reaction due to the formation of oxides compared to Al-5TiC (2 μm) composites. For all TG samples, initially weight loss was noted and followed by an increase in weight. The initial weight loss was due to the desolation, desorption, drying and decomposition of the metal matrix composite. In the Al-5TiC (2 μm) composite, the weight loss takes place up to the temperature of 825°*C*, and followed by weight gain. This may be due to the adsorption, absorption, solid-gas reactions and oxidation reactions. As the metal matrix composite reaches the nano size, the weight gain increases a maximum. This was due to the occurrence of oxidation reaction (equation (1)).

Hardness

Figure 5(a-b) illustrates the effect of the TiC particle size & amount on the composite hardness. Considering this figure, by increasing the amount of TiC, composite hardness increases since its hardness is much higher than that of pure aluminum [24]. It was obtained that by increasing the amount of TiC from 0% to 10%, hardness increased from 32.4 to 43.7*HV*. Obviously, the hardness of aluminum improves considerably with the additions of TiC particles at the expense of

its ductility that can be attributed to higher hardness of TiC. Considering this figure, it illustrates that decreasing the particle size will increase the composite hardness. So, the average hardness of Al–TiC composite specimens with ≤200 nm TiC particles are higher than that of the Al–TiC composite specimens with 2 μmTiC particles. The reason for this increase can be studied from two viewpoints. (i) Due to greater interfacial area between the hard & soft phases. (ii) The defectsin the coarse-grained particles were more than the fine-grained ones which results in its easy fracture under tension.

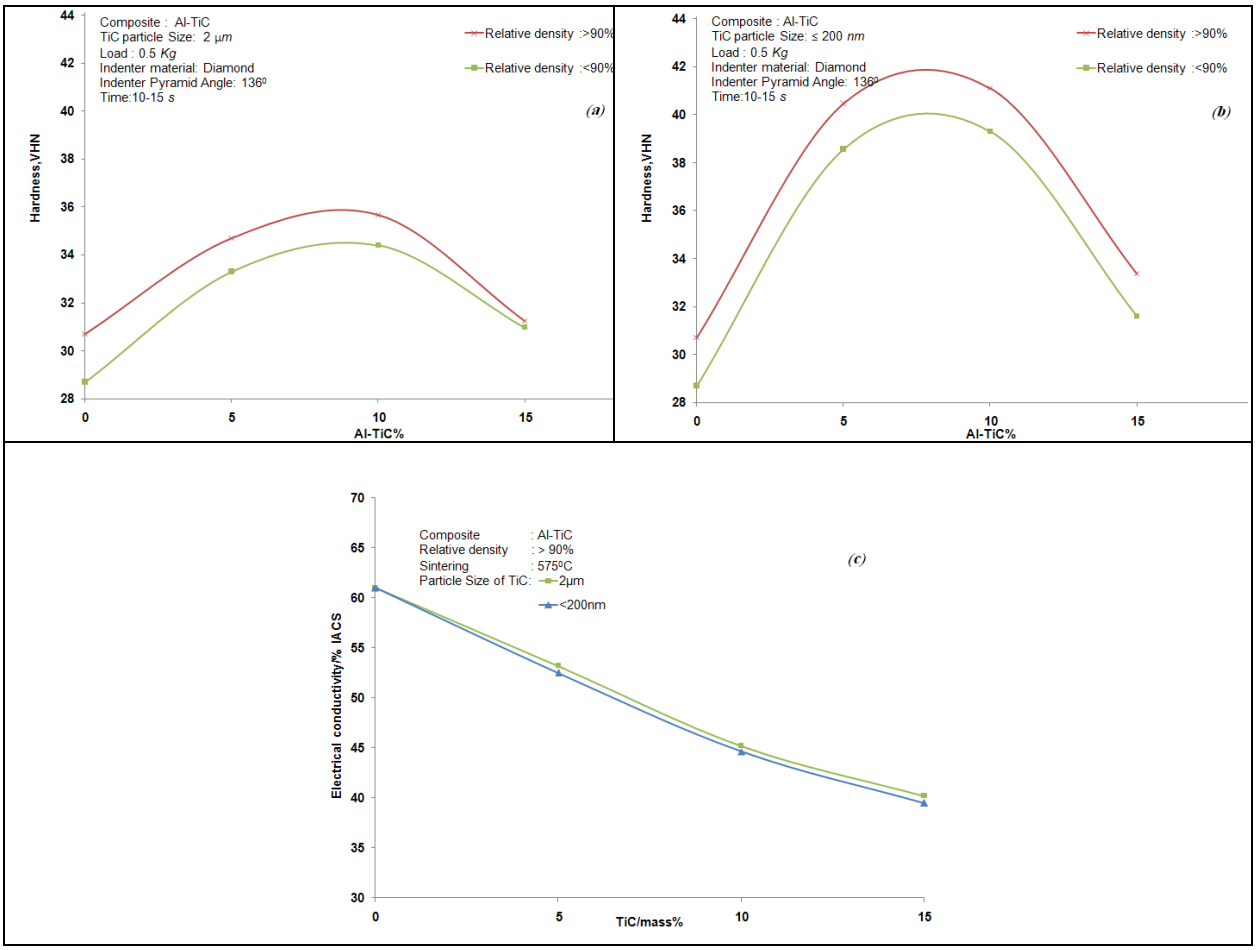

Figure 5: Hardness Value of Composite (a) Al-TiC (2*μm*), (b) Al-TiC (≤200*nm*), (c) Effect on Conductivity on % TiC

Electrical Conductivity

Figure 5(c) illustrates the results of electrical conductivity of Al-TiC composites, produced via compacting method, based on content of titanium carbide with ≤200 *nm*&2 *μm* respectively. The electrical conductivity of composites was decreased with the increase in addiction rates of titanium carbide. While the electrical conductivity of Al with no addition was measured as 61% IACS, the electrical conductivity of aluminium matrix Al-TiC (2 *μm*) composites with 5, 10 and 15%TiC addition were measured as 53.2, 45.2 and 40.2% IACS, and the electrical conductivity of aluminium matrix Al-TiC (≤200 *nm*) composites with 5, 10 and 15%TiC addition were measured as 52.5, 44.6 and 39.5% IACS, respectively. The above results exhibits low electrical conductivity of pure Al [25]. Interaction between free electrons and nucleus are weak in the metals. Therefore, electrons easily move and accordingly electrical conductivity of metals is good. However, electrons do not move, as the electrons are firmly bonded to the nucleus in the carbides. For this reason, electrical conductivity of carbides are weak [26-27]. Increasing addition of TiC in Al matrix results in reduction of

electrical conductivity as a result of inhibition of Al electrons movements. The reduction of electrical conductivity with increasing the TiC content may be due to high electrical resistivity of TiC, and the density of dislocations between TiC&Al matrix increases. Increased dislocation density intensifies the scattering of electrons on interface Al-TiC, resulting the decreases in electrical conductivity. And finally, the attendance of TiC can efficiently purify the grains of Al-TiC composite [28]. Further observation indicates that, the electrical conductivity in the Al-5%TiC (≤200 *nm*) composites shows a slight reduction compared to Al-5%TiC (2 *μm*) because the strength and hardness of the composites increase with the increasing amount and size variation of particle reinforcement.

Effect of TiC Particle Size Variation on SWR

Figure 6 (a-d) illustrates the difference of specific wear rate (SWR) with standard load at different sliding distance and at a constant sliding velocity of 2.61 m/s for pure Al & with different particle sizes of TiC at 5, 10 and 15% (≤ 200 nm, 2 μm) of the composites respectively. It is analyzed that the SWR increases gradually with increasing standard load& sliding distance. This is due to the formation of scratches, grooves and debris. Further, it was found that the SWR of the composites is lower than that observed in pure Al and decreases with increasing volume fraction & particle size reduction (≤ 200 nm) of the TiC in the composite is evident from Figure 6(b-d). The curve fitting technique was used to analyze the Polynomial and power law equations of different composites [29]. After analyzing the equation, it was found that Regression coefficient (R^2) values for the polynomial equations are greater than the power law equations and also shows that if the R^2 value is 1, then there is no difference between the experimental and the predicted value. The polynomial equations provide accurate conformity. Further, the number of experiments can be minimized by using regression polynomial equation (Table 3).

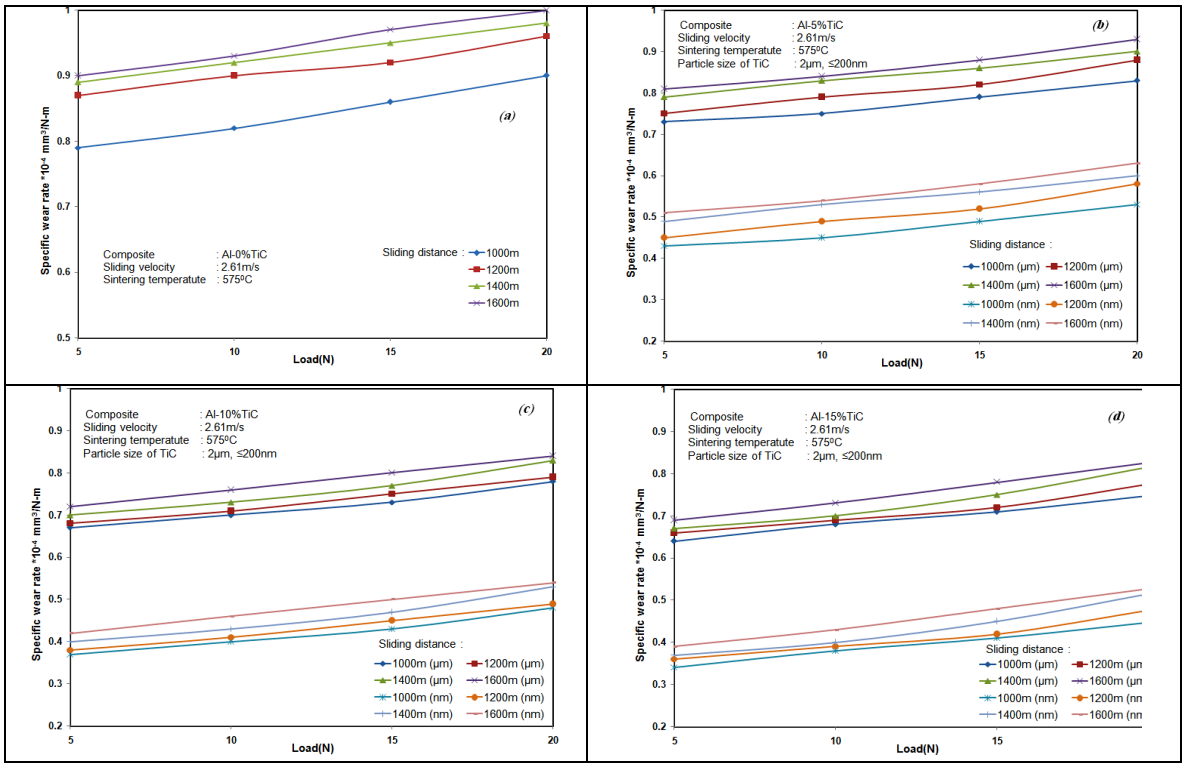

Figure 6: (a-d) Effect of Specific Wear Rate as a Function of Normal Load with Various Sliding Distance at Different Particle Size

Table 3: Curve Fitting Results: Specific Wear Rate Vs Normal Load

Composite	Polynomial Equation	R^2	Power Law Equation	R^2
Al-0TiC	$Y=0.006x+0.865$	0.996	$Y=0.791x^{0.075}$	0.958
Al-5TiC	$Y=0.000x^2+0.003x+0.79$	1	$Y=0.687x^{0.095}$	0.918
Al-10TiC	$Y=0.008+0.68$	1	$Y=0.599x^{0.108}$	0.969
Al-15TiC	$Y=0.000x^2+0.006x+0.652$	0.999	$Y=0.552x^{0.13}$	0.950

Figure 7 (a-d) shows the variation of SWR with standard load at different particle sizes of TiC at 5, 10 and 15% (≤ 200 nm and 2 µm) of the composites and at a constant sliding velocity of 2.61 m/s for different sliding distances respectively. It is analyzed that the SWR increases gradually with increasing standard load. The SWR decreases gradually as the volume fraction of TiC increases and decreases in the TiC particle size. Thereafter, an improvement in hardness, high bonding and reduction in real area of contact was found out by the incorporation of hard TiC particles. Since real area of contact was found out due to the ratio of the load to the hardness of the pin material. Therefore, as a result SWR decreases with decreasing real area of contact. Figure 7 (a-d) describes the trend for both Al-TiC particles (2 µm, ≤ 200 nm), but the Al-TiC (≤ 200 nm) composite provides less SWR than the Al-TiC (2 µm) composite. This is due to the developed oxide layer.

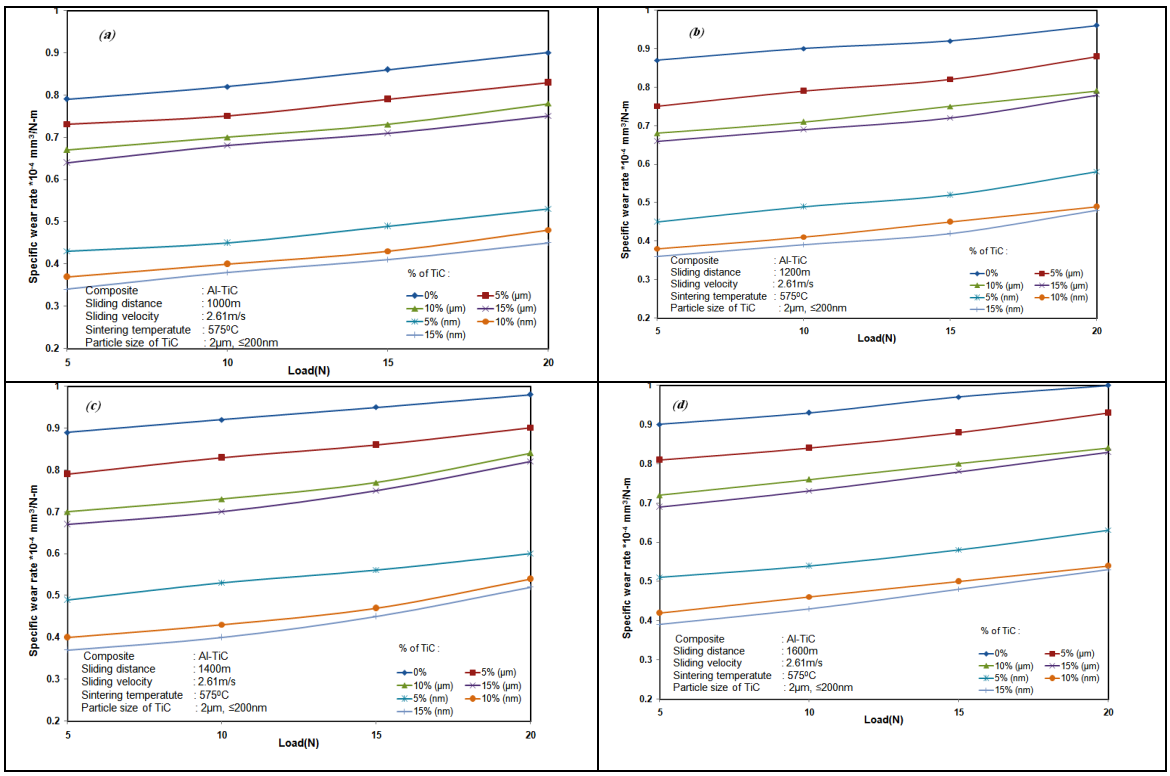

Figure 7: (a-d) Effect of Specific Wear Rate as a Function of Normal Load with wt. % of TiC at Different Particle Size

Effect of Tic Particle Size Variation on COF

Figure 8 (a-d) illustrates the variation of coefficient of friction (COF) with standard load at different sliding distance & at a constant sliding velocity of 2.61 m/s for pure Al&with different particle sizes of TiC at 5, 10 and 15% (≤ 200 nm, 2 µm) of the composites respectively. It reveals that COF increases with increase in sliding distance for all composites. Al-15% TiCcomposite has the lowest COF due to the fine asperities. The weight loss is less as the hard nature of the material. The smart harshness take the developed heat from the surface. It confirms that the initially noted COF is

low and shows if the harshness are strong and rigid, it leads to develop high heat level at the surface along with an increment of COF. The pure Al has high COF compared to the other composites due to the formation of thick tribo layer, which leads to increase in temperature as is evident from Figure 8(b-d). Further, analyzing it was found that, Since the higher hardness of the composite appearing in minor real area of contact has smaller number of junctions which need smaller energy to get sheared during sliding as compared to the Al-TiC (2 µm) composites. And it leads to trend for both Al-TiC particles (2 µm, ≤ 200 nm), in which Al-TiC (≤ 200 nm) composite provides less COF than the Al-TiC (2 µm) composite.

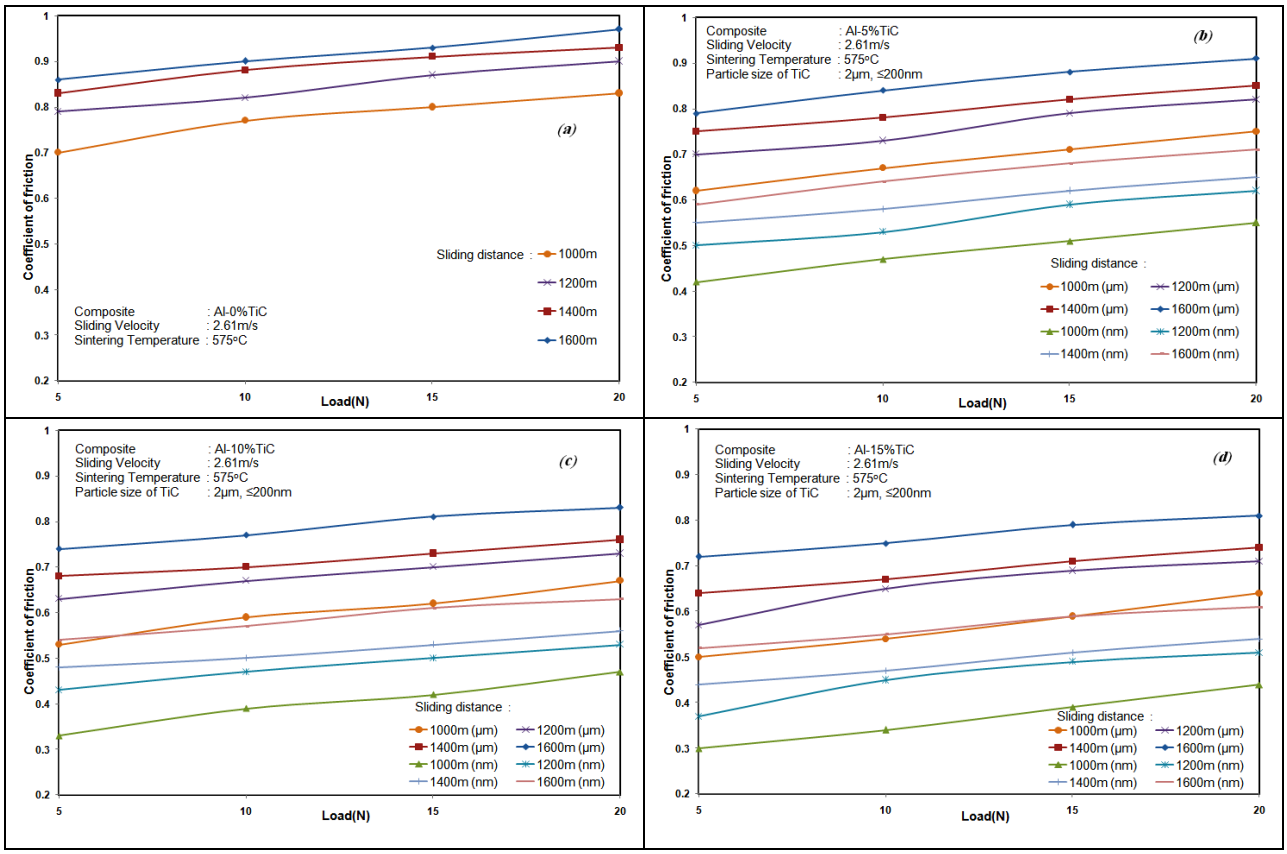

Figure 8: (a-d) Effect of Coefficient of Friction as a Function of Normal Load with Various Sliding Distance at Different Particle Size

Figure 9 (a-d) shows the variation of COF with standard load at different particle sizes of TiC at 5, 10 and 15% (≤ 200 nm and 2 µm) of the composites and at a constant sliding velocity of 2.61 m/s for different sliding distance respectively. It is examined that the COF increases gradually with increasing normal load. While it decreases gradually as the volume fraction of TiC increases and decreases in the TiC particle size. As the load increases, the contact surface becomes higher and hence the heat generation increases with the increase in the COF& comparatively COF decreases in the steady state. It is noted, that while increase in the volume fraction of TiC content, the part of the TiC on the sample surface increases, and therefore they act as a shielding while doing the wear test, and thus they contribute to the decrease of coefficient of friction. In other words, it states that the TiC reinforcement has deeply penetrated in to the soft matrix material to reduce the friction coefficient. During sliding, the TiC can cover the wear surface and act as obstacles which decreases the coefficient of friction.

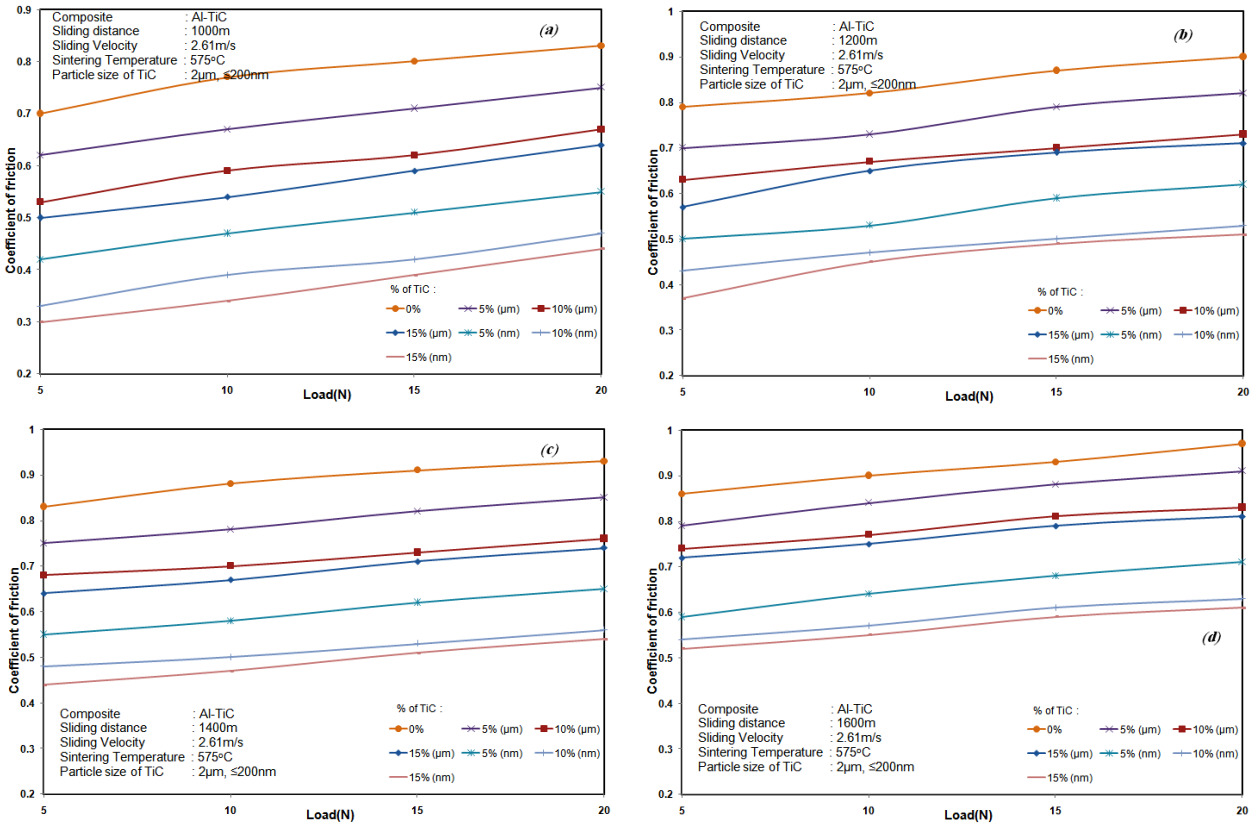

Figure 9: (a-d) Effect of Coeffient of Friction as a Function of Normal Load with wt. % of TiC at Different Particle Size

Effect of TiC Particle Size Variation on Wear Worn Surface

The SEM analysis of the worn surface of the Al-TiCnano composites are shown in Figures 10(a-d). Figure 10(a) illustrates the SEM image of pure Al. It depicts severe adhesive wear in the specimen. Furthermore it also shows that ploughing of metals appearing equivalent to the sliding direction. When the disc contact the sample, the hard counter steel body contracts the Al specimen, so that the friction coefficient & wear loss becomes higher. The ploughing of metal Can be done due to the direct contact between the specimen & steel counter disc. This was used by the hardened wear debris from Al. Figures. 10(b-d) shows that the worn surface of Al with 5,10, and 15 wt. % of TiC(≤ 200 nm). It is smoother than that of the Al. The hard ceramic particles are very much harder than the Al matrix and thus, better wear resistance can be attained. Moreover, with an increase in the TiC (≤ 200 nm) content, the worn surfaces of the composites become smoother.

For the TiC(≤ 200 nm) particles, due to better micro ploughing& lower wear rate of the composites, can act as a shield, and protect the Almatrix from the plastic deformation. As the TiC(≤ 200 nm) content increases, the conflict to the penetration of the ceramic particles is enriched, leading to the better wear resistance. It can also be noticed from the Fig. 6(b-d), that the wear rate of the Aland composites increases with increasing the load. While the applied load increases from 5*N* to 20 *N*, the worn surface of the Al specimen becomes rougher, as shown in Fig. 10(a). When the TiC(≤ 200 nm) was incorporated to the Al composites the worn surface becomes smoother, as exposed in figures. 10(b-d). During the wear test the applied load is relatively large, the ceramic particles are squeezed from the Al matrix, and acts as a shielding throughout the test. Figure 10(c) shows the worn surface of the 10 wt.% of TiC(≤ 200 nm) reinforced with Al composite is completely protected by the hard ceramic particle, it is also noted that the smooth grooves were formed in the composites.

More over, the addition of 10 wt.% of TiC(≤ 200 nm) particles to the Al matrix considerably increases the hardness in composite with minimization of the plastic deformation. In this condition, the wear loss of the composite is reduced, while adding TiC(≤ 200 nm), which may act as shielding layer during sliding, than other composites.

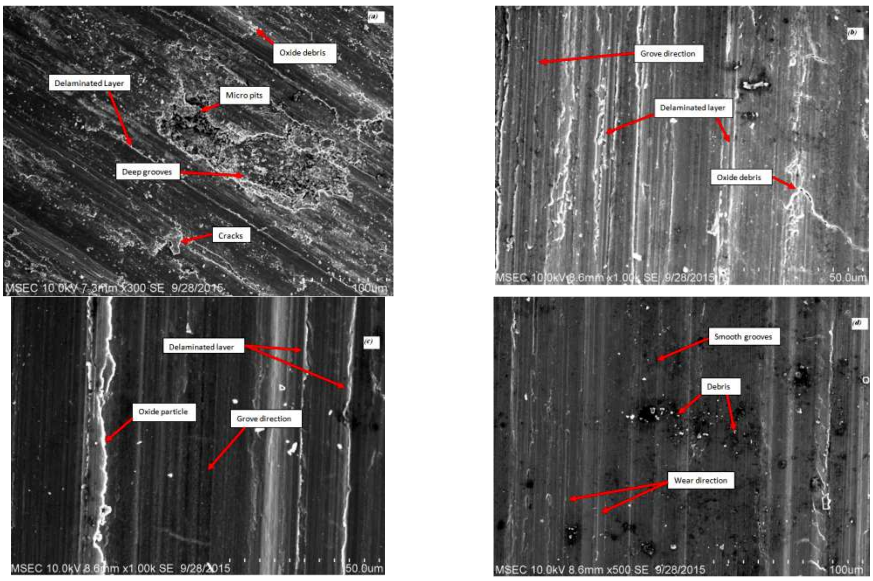

Figure 10: (a-d) SEM Micrograph of a Worn Surface after Wear Test of Various Composites (≤200nm) (a) Al (b) AL-5TiC (c) Al-10TiC (d) Al-15TiC

Figure 11 (a-c) shows that the worn surface of Al with 5,10, and 15 wt. % of TiC (2µm). The formations of the plots are similar to the figures10(b-d). It is also noted from the figures10&11, exhibits that the pore size becomes largerwith increasingTiC content (2µm) and hence the SWR value increases. Figure 10 & 11 describes the nature of both Al-TiC particles (2 µm, ≤ 200 nm), where Al-TiC (2 µm) composite isless smooththan the other composite because of its dense packing.

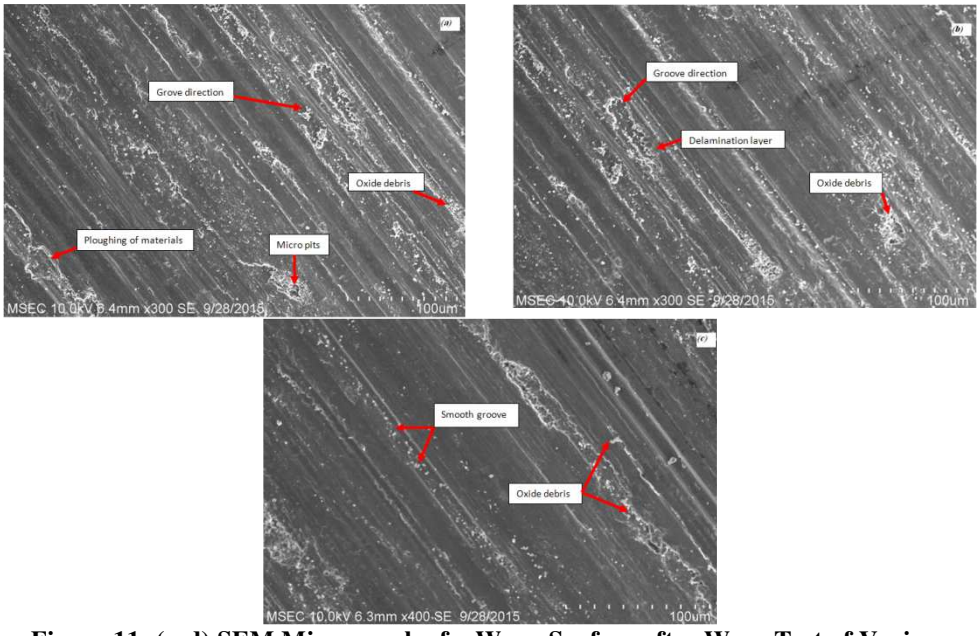

Figure 11: (a-d) SEM Micrograph of a Worn Surface after Wear Test of Various Composites (2µm) (a) Al (b) Al-5TiC (c) Al-10tic (d) Al-15TiC

CONCLUSIONS

Based on the experimental investigations of the different particle size (≤ 200 *nm*& 2 *μm*) of titanium carbide particles at different loads (5, 10, 15 & 20 *N*) & at different sliding distances(1000, 1200, 1400 & 1600 *m*), the following conclusions are drawn:

- DSC result shows quick phase transition for nano powder & therefore mass loss event during the decomposition at the earlier stage. Further, it was found that the during decomposition, the change of enthalpy affects by particle size reduction of TiC.
- Hardness value increases with increasing the secondary particle TiC in the Al matrix.
- For a given load, there is a linear increase in SWR of composites and pure aluminium pinswith sliding distance under dry sliding.
- The SWR increases gradually with increasing normal load. However, compared to pure aluminium, composites have exhibit low wear rate. This may be, due to incorporation of hard TiC particles appearing in a minor real area of contact, ascribed to higher hardness of the composite and therefore, SWR. SWR also decreases gradually with increase in volume fraction and particle size reduction of titanium carbide.
- The coefficient of friction for the load of 20 *N* was greater than those for the loads of 10 *N*& 15 *N* at constant sliding velocity. However, the coefficient of friction increases as the sliding distance increases.
- Analyzing worn surface morphology, it was concluded that the pin surfaces are damaged by the cause of such wear mechanisms as abrasion, delamination and oxidation. Among these mechanisms, abrasion and delamination predominates at a sliding distance of 1600*m*.
- The addition of nano sized TiC particles as reinforcement in Al matrix was established to embellish the wear resistance significantly.

REFERENCES

1. *VelusamySenthilkumar, BidwaiUday, Omprakash,"Effect of titanium carbide particle addition in the aluminium composite on EDM process parameters", Journal of Manufacturing Processes, vol.13, pp. 60-66, 2011.*
2. *RajneshTyagi,"Synthesis and tribological characterization of in situ cast Al-TiC composites", Wear, vol. 259, pp. 569-76, 2005.*
3. *S. Murphy, R. Arikan,"Anisotropic wear of planar-random metal matrix composites with zinc alloy matrix", Wear, vol.155, pp.105–15,1992.*
4. *Y Sahin, S. Murphy,"The effect of fibre orientation on the dry sliding wear of borsic-reinforced 2014 Al alloy", J. Mater. Sci, vol.31, pp. 5399–407, 1996.*
5. *S. F. Moustafa,"Wear and wear mechanisms of Al-22%Si/$A1_2O_3$ composite"*
6. *Wear, vol.185, pp.189–95, 1995.*
7. *A. P. Sannino, H. J. Rack,"Tribological investigation of 2009 Al-20 vol.% SiC_p/17-4 PH Part II: counterpart performance", Wear, vol.189, pp.1–20, 1995.*

8. *Viswa Mohan Pedagopu, Hybrid Modelling, Manufacturing of Mold Tool and Plastic Flow Analysis of an Air Cooler Tank, International Journal of Mechanical and Production Engineering Research and Development (IJMPERD), Volume 3, Issue 3, July - August 2013, pp. 109-116*

9. *S. Wilson, A. T. Alpas,"Wear mechanism maps for metal matrix composites", Wear, v ol.212, pp.41–49, 1997.*

10. *Du Jun, Liu Yao-hui, Yu Si-rong, Li Wen-fang,"Dry sliding friction and wear properties of Al_2O_3 and carbon short fibresreinforced Al–12Si alloy hybrid composites" Wear, vol.257, pp. 930–40, 2004.*

11. *T. Choh,"Fabrication and mechanical properties of in situ formed carbide particulate reinforced aluminium composite", in: M. K. Surappa, (Ed.), Proc.of Inorganic Matrix Composites, TMS, Warrandale. PA, pp.31-39, 1996.*

12. *M. Roy, B. Venkatraman, V. V. Bhanuprasad, Y. R. Mahajan, G. Sundarajan,"Dry sliding wear behaviour at ambient and elevated temperatures of plasma transferred arc deposited aluminium composite coatings". Metall. Trans. A, vol.23A, pp. 2833-47, 1992.*

13. *SonerBuytoz, FethiDagdelen, SerkanIslak, MedihaKoK, DurmusKir, ErcanErcan,"Effect of the TiC content on microstructure and thermal properties of Cu-TiC composites prepared by powder metallurgy", J Therm Anal Calorim, vol.117, pp.1277–83, 2014*

14. *P. Figiel, W. Biedunkiewicz, D. Grzesiak,"Oxidation process of the steel/nc-TiCnanocomposites", JTherm Anal Calorim, vol.108, pp.979-83, 2012.*

A. *Azhagurajan, N. Selvakumar, JeyakumarSriram,"Flame analysis of micro and nano flash powder for firework applications", J Pyrotech, vol. 30(2), pp.11–21, 2011.*

A. *Azhagurajan, N. Selvakumar, M. Mohammed Yasin, "Minimum ignition energy for micro and nano flash powders", Process SafProg, vol.31(1), pp.19–23, 2012.*

15. *S. Basavarajappa, G. Chandramohan, J. Paulo Davim,"Application of Taguchi techniques to study dry sliding wear behaviour of metal matrix composites", Mater Des, vol. 28, pp. 1393-98, 2007.*

16. *B. Selvam, P. Marimuthu, R. Narayanasamy, V. Anandakrishnan, K. S. Tun, M. Gupta, M. Kamaraj,"Dry sliding wear behaviour of zinc oxide reinforced magnesium matrix nano- composites", Mater Des, vol.58, pp. 475-81, 2014.*

17. *M. Sivaraj, N. Selvakumar,"Experimental Analysis of Al-TiC Sintered Nano Composite on EDM Process Parameters Using ANOVA", Mater. Manuf. Process, vol.31, pp. 802-812,2016.*

18. *V. Senthilkumar, A. Balaji, HafeezAhamed,"Effect of secondary processing and Nanoscale reinforcement on the mechanical properties of Al-TiC composites", Journal of Minerals and Materials Characterization and Engineering, vol.10, pp. 1293-306, 2011.*

19. *K. Preetha Nair, Paulbert Thomas, Rani Joseph. "Latex stage blending ofmultiwalled carbon nanotube in carboxylated acrylonitrile butadienerubber: mechanical and electrical properties", Mater Des, vol.41, pp.23–30, 2012.*

20. *ASTM E1004-02, "Standard practice for determining electrical conductivity using the electromagnetic (eddy-current) method".*

21. *S. Suresh, N. ShenbagaVinayagaMoorthi, S. C. Vettivel, N. Selvakumar,"Mechanical behavior and wear prediction of stir cast Al–TiB_2 composites using response surface methodology", Materials and Design, vol. 59, pp. 383–96, 2014.*

22. *K. Williamson, W. H. Hall, "X-ray line broadening from aluminium and wolfram", ActaMetallurgica, vol.1, pp.22-31, 1953.*

23. *Omyma El-Kady, A. Fathy,"Effect of SiC particle size on the physical and mechanical properties of extruded Al matrix*

nanocomposites", Mater Des, vol. 54 pp.348–353, 2014.

24. *S. C. Vettivel, N. Selvakumar, R. Narayanasamy, N. Leema,"Numerical modelling, prediction of Cu–W nano powder composite in dry sliding wear condition using response surface methodology", Mater Des, vol.50, pp.977–96, 2013.*
25. *S. F. Santos, M. C. De Andrade, J. A. Sampaio, A. B. Da Luz, T. Ogasawara,"Thermal study of TiO_2-CeO_2 yellow ceramic pigment obtained by the pechini method", J Therm Anal Calorim, vol. 87(3), pp.743–6, 2007.*
26. *M. Schoentiz, B. Patel, O. Agboh, E. L. Dreizin,"Oxidation of aluminium powders at high heating rates"ThermochimActa, Vol.507-508, pp.115-22, 2010.*
27. *H. O. Pierson,"Handbook of refractory carbides and nitrides. Noyes: William Andrew"1996.*
28. *Q. Z. Wang, C. X. Cui, D. M. Lu, S. J. Bu,"Fabrication and properties of a novel Zno/Cu composite", J Mater Process Technol, vol.210, pp.497-503, 2010.*
29. *N. Selvakumar, S. C. Vettivel,"Thermal, electrical and wear behaviour of sintered Cu-W nanocomposites", Mater Des, vol.46, pp.16-25, 2013.*